Metallic nanoislands: preferential nucleation, intermixing and electronic states

A L Vázquez de Parga, J M Gallego, J J de Miguel and R Miranda

Departamento de Física de la Materia Condensada, Instituto de Ciencias de Materiales 'Nicolás Cabrera', Universidad Autónoma de Madrid, Cantoblanco, Madrid 28046, Spain

Abstract
A fairly common phenomenon is intermixing during growth. The surface is an efficient strain reliever and in many cases the islands that appear on the surface upon deposition do not contain the deposited material, but rather they consist of atoms ejected from the substrate. This is illustrated by the Fe/Au(100) system, where the local spectroscopic characteristics of the STM are employed to visualize the chemical composition of the islands and demonstrate that they are made out of Au atoms.

Computer simulations, either Monte Carlo or molecular dynamics, that use realistic interatomic potentials can often reveal the complex processes that occur during deposition. The simulations have shown novel processes of intermixing taking place during the growth of Co on Cu(111): two-dimensional islands larger than a critical size 'explode', etching the substrate and forming several-layers-high, three-dimensional islands. These islands are triangular with two different orientations depending on whether or not they present a stacking fault at the Co/Cu interface, as indicated by quantitative LEED analysis. STM spectroscopy reveals that it is much easier to inject electrons on the islands with a faulted Co/Cu interface. This might be relevant to improve the performance of recently developed spin-valve transistors, where the reduced electron transmission across the Co/Cu metal base represents an important practical problem. In this respect, the different electronic states of fcc and hcp-stacked Co islands grown on Cu(111) can be detected locally with STM spectroscopy and compared with calculated local density of states (LDOS). The fcc-stacked Co films show higher transmission and larger LDOS in the empty states. The use of surfactants to modify the growth of the Co films could allows us to enhance the electron transmission and, thus, the efficiency of these transistors.

(Some figures in this article are in colour only in the electronic version)

1. Introduction

The burgeoning field of spin electronics or 'spintronics' refers to electronic devices in operation of which the direction an electron spin is pointing is just as important as the electron charge. The related magnetic nanostructures are attracting an increasing interest: magnetic multilayers, wires and, more recently, magnetic quantum dots are the subjects of intense research. Both new physics and applications are the driving forces behind this. For instance, an increasing number of devices that exploit spin-polarized transport (reading heads, magnetic field sensors, magnetic random access memories, metal base or semiconductor field-effect transistors) have been proposed or built based on magnetic multilayers [1]. Some of these devices take advantage of physical effects, such as the giant magnetoresistence (GMR) [2] or the tunnelling magnetoresistence (TMR) [3], which depend on the spin-dependent flow of the electrons with energies at the Fermi level. Others, such as the spin-valve transistors [4, 5], rely on the ballistic transport of hot electrons with energies 1–2 eV above the Fermi level [6] across a Co/Cu multilayer which constitutes the base region of the transistor. The two-component intrinsic nature of spintronic devices based on laterally ordered magnetic quantum dots might even allow quantum computing in the solid state at room temperature.

There are different approaches to the fabrication of ordered nanostructures on a surface. One of them involves the preferential nucleation of islands on a regularly distributed lattice of nucleation sites, taking advantage of the fact that some surfaces (e.g. Au(111) or (100)) naturally present a lattice of dislocations that serve as nucleation centres for the deposited atoms in a certain temperature window [7]. The drive to construct metallic nanostructures with well defined properties requires a detailed understanding of the various atomic processes that occur during the formation of nanosized islands on surfaces. Increasing evidence has been accumulated in the past few years indicating that surfaces are not simply a static scenario onto which the deposited atoms diffuse and nucleate [8]. In particular, it has been found that intermixing during deposition is far more common that previously expected [9]. It is thus essential to explore the limits imposed by intermixing in the objective of growing magnetic nanostructures on surfaces. To this end it is crucial to develop a multitechnique approach that employs new methods of growth, realistic computer simulation, local spectroscopies and accurate structural techniques. This paper reports some results of such an approach.

2. Results and discussion

2.1. Single-atom intermixing

The richness of atomic processes that occur during crystal growth has been recently revealed in all its complexity by the images provided by the STM. Figure 1 illustrates the case of the first stages of the deposition of a magnetic metal, Fe, on a non-magnetic, metallic substrate, Au(100). Many different types of island, large and small, elongated along the 'rows' of the '5 × 1' reconstruction and almost square, have appeared on the surface. There are two domains of the reconstruction rotated through 90°, which may or may not change upon crossing the steps; there is material added to some of the atomic steps, but not to the others. What is the composition of the islands? Are they made of Fe, Au or some mixture? composed of the ejected Au atoms. When the Au island covers a critical number of Fe atoms it does not reconstruct, while if it is located over unperturbed substrate it is reconstructed.
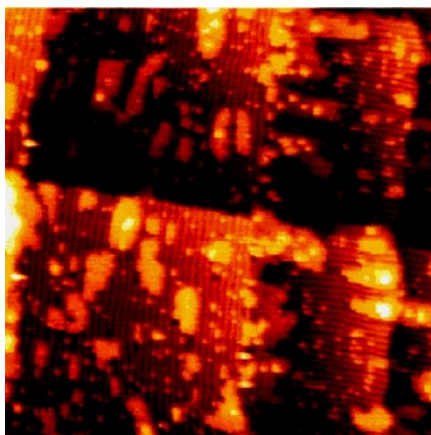
Figure 1. STM image of 0.16 ML of Fe deposited on Au(100) at 300 K with a rate of 1.2×10^{15} atoms min^{-1}.

2.2. Collective intermixing

In certain cases, particularly for growth on *soft* metallic substrates, new forms of intermixing are possible. The initial growth of Co on Cu(111) is one of these cases. The deposition of Co at 300 K on Cu(111) produces some characteristic features: triangular islands with bilayer height and two different orientations [16, 17], decoration of the steps [18] and etching of the substrate [19] with appearance of mobile vacancy islands. STM images, such as shown in figure 2, reveal the morphology of a film deposited at 370 K that presents the same phenomenology as those grown at 300 K except for the more frequent appearance of islands three and four layers high.

Computer simulations, either Monte Carlo (MC) or molecular dynamics (static relaxation), that use realistic interatomic potentials fitted to bulk and surface properties [20], can often reveal the complex processes that occur during deposition on a realistic timescale [21]. According to the MC simulations reproduced in figure 3, the Co atoms diffuse over the Cu(111) terraces by *hopping* without intermixing with the Cu substrate and with a very small diffusion barrier. In contrast, step crossing occurs by *exchange* with the Cu atoms at the steps. Co atoms arriving at a descending step push Cu atoms out of it and take their place, becoming immobile. The next Co atom approaching the step is captured by a potential well, 0.24 eV deep according to static relaxation calculations [21], which develops at the position of the Co-replaced Cu atom. This gives rise to preferential nucleation and the observed [18] decoration of the steps. The wires formed this way, however, contain a mixture of Co and Cu, whose magnetic properties are probably not homogeneous, since the alloying process is random in nature. Different experimental techniques, such as tunnelling spectroscopy and CO decoration and subsequent visualization with the STM can detect the presence of both Co and Cu in the wires.

The computer simulations have also shown novel processes of collective intermixing taking place during the growth of Co on Cu(111): two-dimensional Co islands larger than a critical size 'explode', etching the Cu substrate and forming several-layers-high, intermixed, three-dimensional islands. Snapshots from the simulations shown in figure 4 indicate that the instability of the Co island starts at the centre of the island, that rises, pulling atoms from the underlying Cu substrate; this deforms until a three-dimensional cluster containing Co *and* Cu develops. Some vacancies are left on the surface.
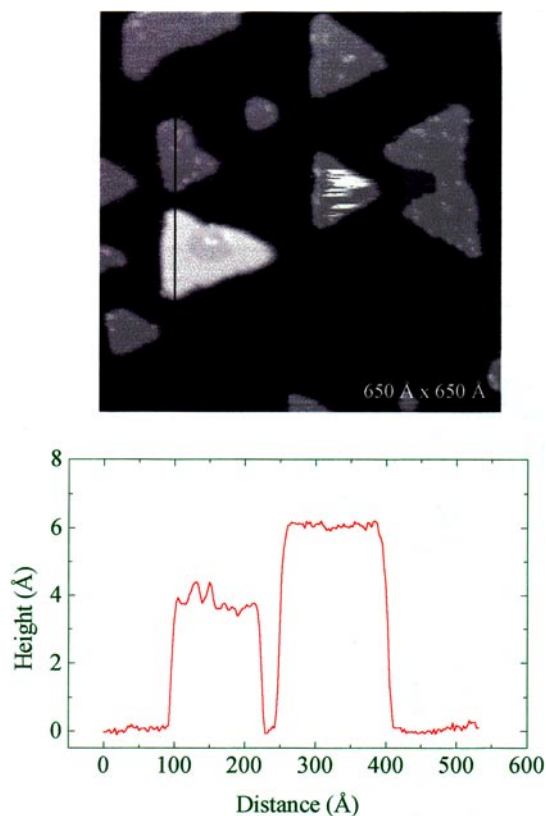
Figure 2. STM images recorded at 370 K after deposition of Co on Cu(111).

There is a critical size for substrate etching: a two-dimensional island of only 21 Co atoms breaks up forming a three-dimensional cluster, but it is not capable of etching Cu atoms from the substrate. The distortion of the substrate is also essential: in simulations where the upper Cu atoms are not allowed to move upwards, the breakup of the Co island does not occur. The effect is probably of elastic nature and takes place in an attempt to decrease the tensile strain of the islands at the cost of the deformation of the substrate. It occurs for Fe/Cu(111) [22] and Co/Au(111) [23], but it is not observed for deposition on mechanically 'hard' substrates such as W(110) [24], Ru(0001) [25] or even Co deposited on 1 ML of Cu/Pt(111).

A first method to detect whether intermixing is taking place during deposition is based on counting how many islands of a given size are present on the surface after deposition. Without intermixing, the shape of the (normalized) distribution of island sizes is a universal function of the size of the critical nuclei [10], since there is only one critical length in the problem. In contrast, when intermixing takes place there are *two* atomic species moving on the surface: the deposited atoms and those ejected from the substrate. This gives rise to a distribution of island sizes with two peaks: there are many very small islands and then an important number of much larger islands. This distribution is very different from the standard island size distribution [10] and it is known as bimodal. The initial growth of Fe on Au(100) [11–13] provides a representative example of such a bimodal distribution. Figure 5 reproduces some typical STM images and the corresponding island size distributions. At the lowest coverages (0.02 monolayers (ML)) the two-peaked distribution can be clearly seen. As more Fe is
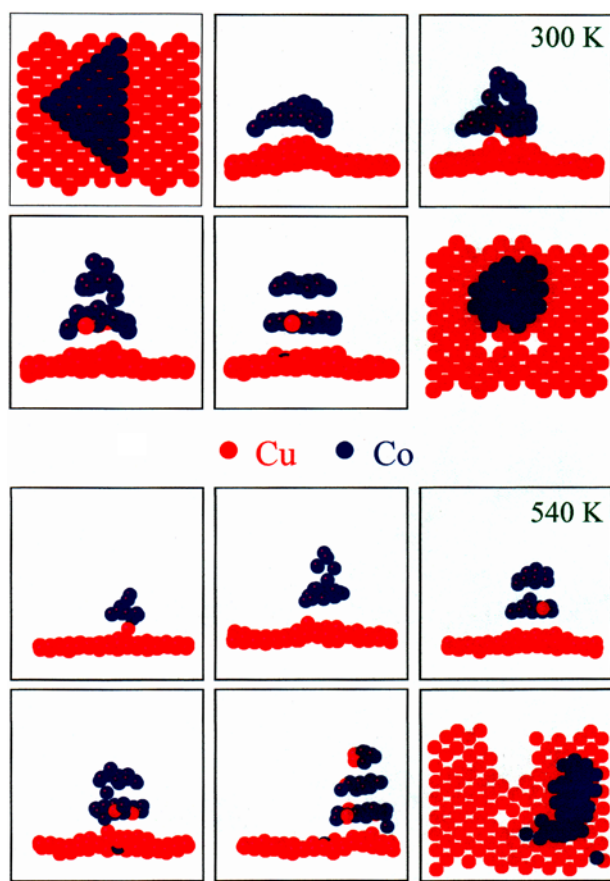
Figure 3. Top and side views of MC simulations showing the 'explosion' of a monolayer-high Co island deposited on Cu(111) at 300 and 540 K. The island contains 28 atoms. The upper panels show the atomic configuration shortly after starting the simulation. Eventually, an island with a mixture of Co and Cu (removed from the substrate) and several atomic layers forms. Notice that a cluster of vacancies appears on the Cu substrate.

evaporated the two peaks coalescence, leaving, however, a long tail extending to large sizes. The same kind of behaviour has been observed in several other systems [14, 15] and it is an indication of intermixing.

The preferential nucleation that occurs (in a given temperature window) at the corners of the reconstructed unit cell of Au(100) is demonstrated by the distribution of distances among the very small islands, which shows maxima at half-integer multiples of the long side of the reconstructed unit cell [12]. Specific nucleation sites also have been found at the elbows of the herringbone reconstruction of Au(111) for Ni, Fe and Co [7]. In all cases the preferential island nucleation requires the initial place exchange of the incoming atoms (Fe, Co etc) at specific sites of the unit cell where the barrier for exchange is smaller and the subsequent preferential nucleation of atoms around these substitutional nuclei.

Kinetic MC simulations illustrate the mechanism of formation of the bimodal distribution and demonstrate that, depending on the conditions, the islands observed on the surface might be composed of the deposited atoms, of the atoms ejected from the substrate by intermixing or of a surface alloy. Figure 6 shows some representative snapshots of the simulations.

(a)

(b)

(c)
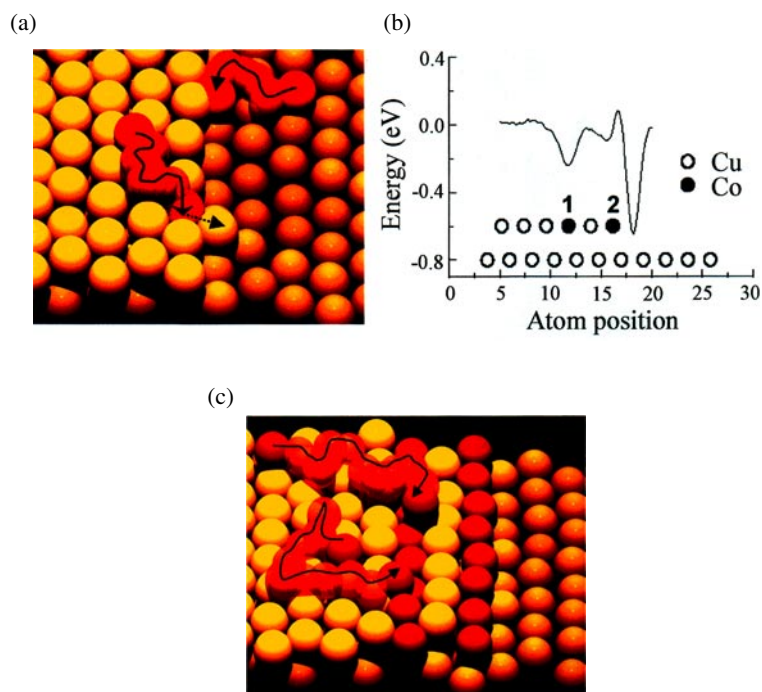
Figure 4. (*a*) MC simulation showing the exchange crossing of a Cu step by a single Co atom. One of the Cu atoms at the step is displaced from its original site by the Co atom approaching the step from the upper terrace. Co atoms arriving at the steps from the lower terrace simply stick to the edge. (*b*) Energy profile for an atom crossing a Co-decorated step and (*c*) three-dimensional rendering of the corresponding MC simulation.

The relevant question to be resolved experimentally is what the composition of the islands that appear at the surface during deposition is. Does Fe or Au form them?

Local spectroscopy on the islands indicates that they are mostly composed of Au. Figure 7 shows that the I–V curves recorded locating the tip of the STM on top of the islands are identical to those obtained on the unperturbed and reconstructed Au(100) surface. They are also identical to those taken on the *unreconstructed* parts of the islands. Furthermore the I–z curves prove that the work function is the same on the islands and on the unperturbed surface.

The STM allows us to find the location of the deposited Fe atoms. By changing the basis of the tunnel junction dark holes of atomic size are detected from -0.4 eV on. The images reveal that the deposited Fe atoms form a random network of isolated atoms embedded within the first layer of the Au substrate. In this case the intermixing takes place upon deposition: each Fe atom moving individually on the surface quickly exchanges place with the Au atoms of the reconstructed surface ejecting (probably three) Au atoms to the outer surface. The Fe atoms remain isolated and immobile, while the ejected Au atoms diffuse on the surface, nucleate and mostly form the large islands.

2.3. Enhanced transmission across faulted Co/Cu interfaces

The transport of electrons across Co/Cu interfaces is crucial to the behaviour of spin-valve transistors. In fact, a severe drawback from the reported spin transistors is the extremely low transmission of electrons 1–2 eV above the Fermi level, that results in severely reduced
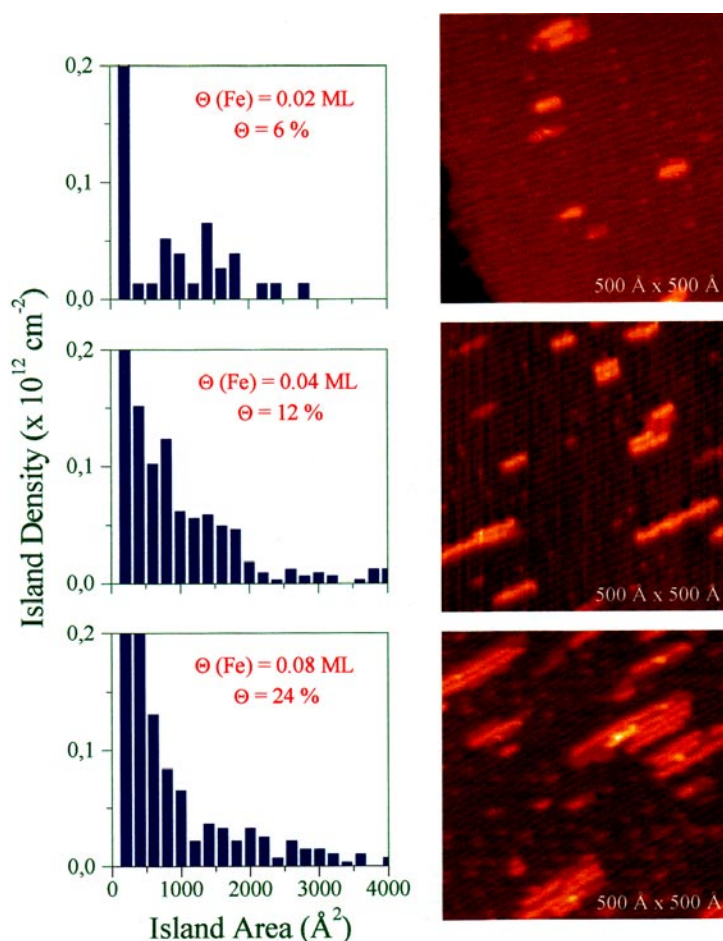
Figure 5. The left-hand panels show the distribution of island sizes for increasing submonolayer coverages of Fe/Au(100) deposited at 300 K. The right-hand panels display some representative STM images (50 nm × 50 nm) corresponding to the same coverages. Notice that the distribution has two peaks, that reflect the preferential existence of small *and* large islands visible in the STM images.

collector currents ranging from 0.05% [4] to 0.004% [5] of the emitter current. A study of the transmission of electrons across Co/Cu interfaces could identify possible solutions.

As indicated above and shown in the upper panel of figure 8, after evaporation of 0.4 ML of Co on Cu(111) at 300 K, there are islands of bilayer height, with triangular shape and two different orientations. It was suggested [16, 17] that the shape and orientation of the Co islands could be rationalized by considering that they nucleate respectively on the two different threefold absorption sites of the surface. Accordingly, while one type of island simply continues the stacking sequence of the Cu substrate, the other presents a stacking fault at the interface. Although at this low coverage standard diffraction techniques lack sensitivity to resolve it directly [26], a recent quantitative LEED study for a *complete* bilayer of Co/Cu(111) [27] identifies that 15% of the Co film indeed presents a stacking fault at the interface, while the rest of the bilayer follows the fcc stacking sequence of the substrate. Thus, the minority islands pointing to the right would form a twin FCC crystallite and have a stacking fault (faulted islands)
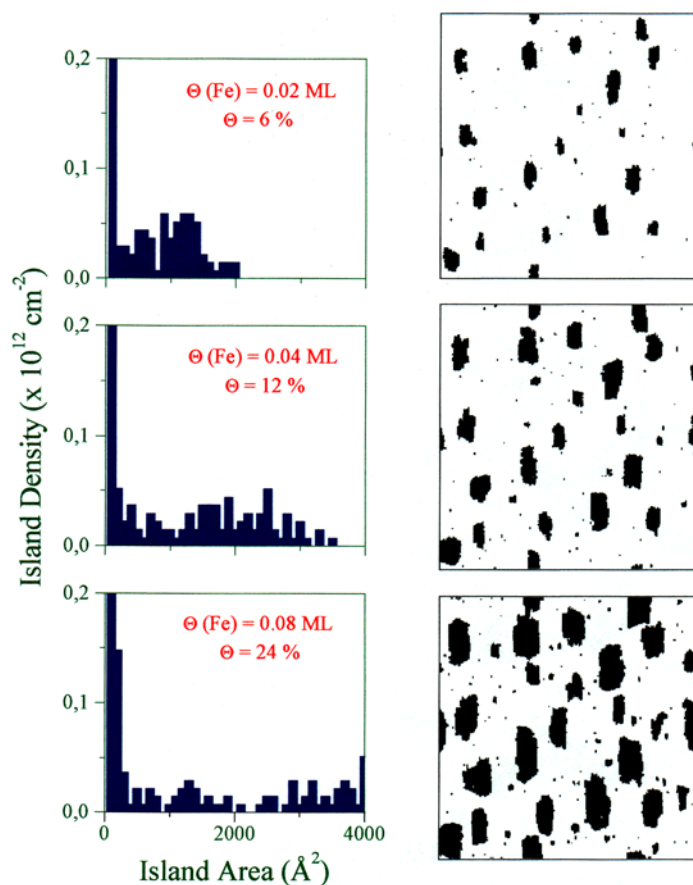
Figure 6. Distribution of island sizes according to the MC simulation for the same coverages of Fe/Au(100) as in figure 5. The panels on the right show some representative snapshots of the simulations. The presence of two diffusing species at the surface (deposited Fe and Au ejected from the substrate by exchange with Fe) is essential to reproduce the bimodal distribution of islands.

at the interface, while the majority islands pointing to the left would simply continue the fcc arrangement of Cu substrate (unfaulted islands).

The lower panel of figure 8 shows two differential tunnelling conductance images at bias voltages sampling the occupied (figure 8(b)) and empty electronic states of the sample (figure 8(c)). The spectroscopic images were measured simultaneously with the constant-current topograph shown in figure 8(a). The tunnelling conductance for both types of island is the same at negative sample bias voltage (occupied states), while it is clearly different at positive sample bias voltage (empty states), with the faulted islands pointing to the right showing larger conductance. Furthermore, the $I-V$ spectra recorded on both islands (not shown [28]) are identical for negative sample bias, but they show higher current on the minority (faulted) islands for any positive bias voltage.

Band structure calculations [28] indicate that the faulted Co islands, in the energy region above the Fermi level, have LDOS projected at 5 A above the surface that is 50% larger than for the unfaulted islands. The corresponding wavefunctions, with d_{xy} and d_{zy} character at the centre of the two-dimensional Brillouin zone, are more delocalized and extend more into the
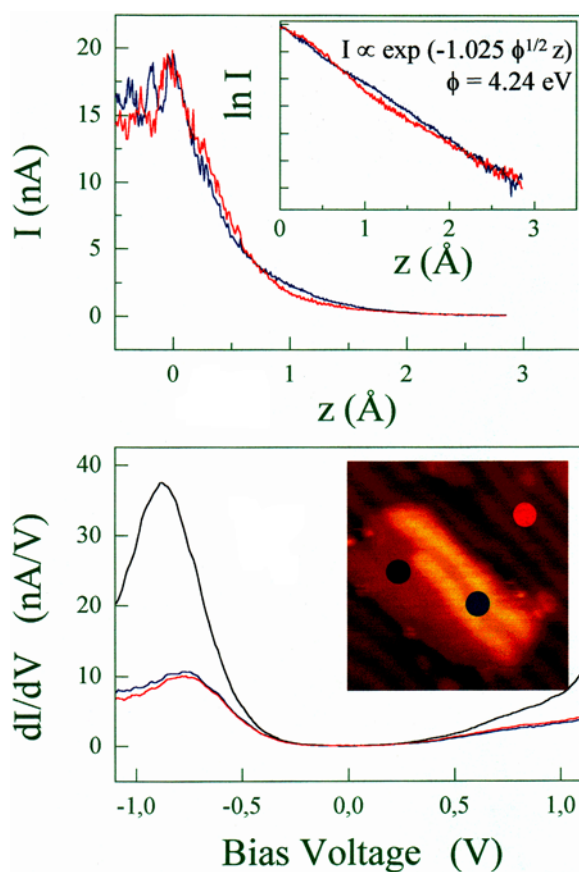
Figure 7. Upper panel: intensity versus distance curves recorded on the reconstructed surface and over an island. Lower panel: tunnelling spectra recorded on different regions of a (partly reconstructed) island that appear on the surface after depositing Fe on Au(100). The inset shows the location within the island where the spectra were taken. The spectrum measured on the reconstructed part of the island is identical to that obtained on the unperturbed, 5×1 reconstructed Au(100) patches. The spectrum measured on the non-reconstructed part of the island is more intense, but otherwise also very similar.

vacuum than their counterparts in the faulted islands. Thus, electrons must be more easily injected in the Co/Cu interface when the tip is placed above a faulted island that when it is above an unfaulted one. Additionally, electrons up to 2 eV above the Fermi level tunnel from the STM tip to Co states with small transverse momentum. Because of the conservation of momentum parallel to the interface many of them are reflected at the interface, since Cu(111) has no propagating momentum states at these energies in the directions lying in a larger cone around the normal than Co [29]. The existence of a stacking fault scatters electrons efficiently into states with different parallel momentum, increasing the transmission across the interface. According to the calculations, the effect should be stronger for minority electrons.

The role of electronic states associated with the stacking fault suggests a possible way to improve the transmission of hot electrons in the energy range 1–2 eV above the Fermi level across Co/Cu interfaces in spin valve transistors: a faulted interface favours the transmission. Now what about the influence of the structure of the rest of the Co film? Although the majority

Topography

40 nm × 40 nm

$(dI/dV)_{V_s}$ V_s = -1.5 V $(dI/dV)_{V_s}$ V_s = +1.5 V
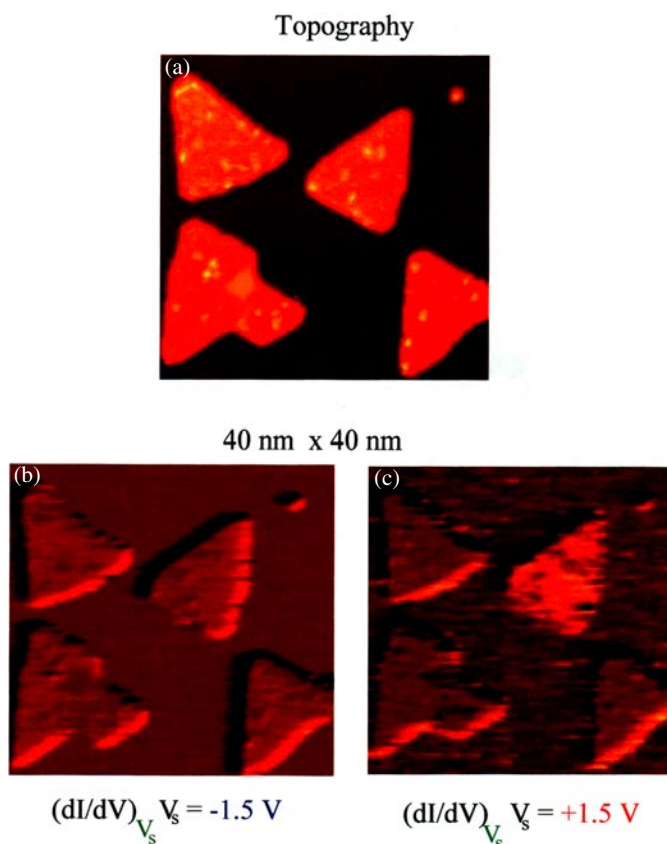
Figure 8. (*a*) (40 nm × 40 nm) topographic STM image of 0.4 ML of Co on Cu(111). Islands with the two types of orientation look identical. (*b*), (*c*) Spectroscopic, dI/dV, images of the same region taken with sample biases of (*b*) −1.5 V and (*c*) +1.5 V. The DC bias was modulated (70 mV) at a frequency higher (8 kHz) than the response of the feedback loop and the AC component of the tunnel current was measured by a lock-in detector. Bright areas correspond to higher differential conductance.

islands of Co continue the fcc stacking sequence of the Cu substrate upon further Co deposition, the film quickly starts to adopt the hcp bulklike structure [30]. In effect, deposited Co atoms from the third layer on choose between the two threefold adsorption sites with almost equal probability. The presence of Ehrlich–Schwoebel barriers to descend steps gives rise to a pyramidal-shaped morphology [31]. On 6 ML thick films the fcc or hcp stacking sequences are simultaneously present as deduced from LEED [30] and surface x-ray diffraction data [32]. Their different electronic structure can be locally identified by STS [29].

Figures 9(*a*) and (*b*) reproduce dI/dV versus V spectra recorded on the upper terraces of different pyramids of a 6 ML thick Co film. Similarly to the islands at the Co/Cu interface, the conductances corresponding to the occupied states are almost identical, but clear differences are seen in the empty states. The fcc structure shows a single peak at 0.5 eV, much larger than the double peak of the hcp phase. Recently, spin-resolved inverse photoemission data [33] have identified the unoccupied surface state on hcp Co(0001). The majority component is located at 0.24 eV above the Fermi level while the minority component is at 0.9 eV, in excellent agreement with the STS data for hcp films. In panels (c) and (d) of the same figure we reproduce the calculated total LDOS around the centre of the Brillouin zone for a Co film with
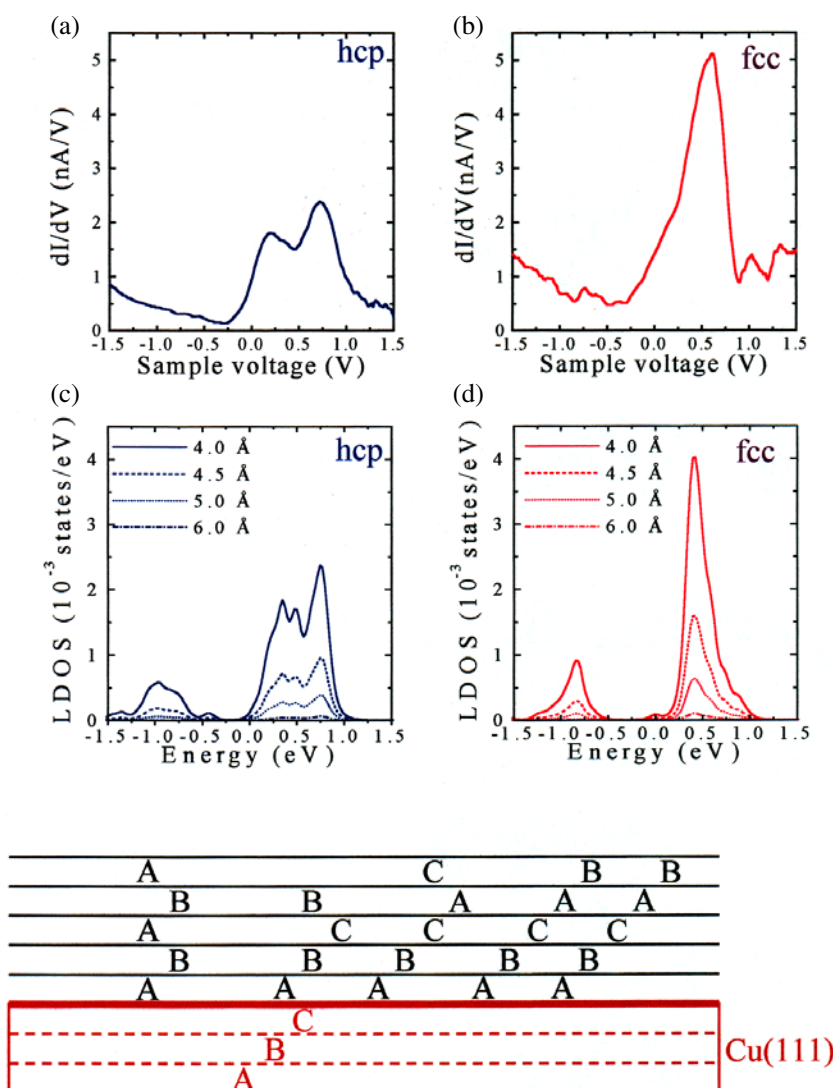
Figure 9. (*a*), (*b*) Tunnelling spectra recorded over differently stacked regions of a 6 ML thick Co film deposited on Cu(111) at 300 K. (*c*), (*d*) The calculated LDOS at different distances from the surface for 6 ML thick Co films with the fcc and hcp structure, respectively. The LDOS has been integrated in a circular region around the centre of the Brillouin zone (25% of its size) to properly weight the states that contribute more to the tunnelling current, and smoothed with a Gaussian of FWHM 0.2 eV to simulate the experimental resolution. The lower panel shows schematically the model of the surface stacking sequence obtained from the XRD data.

fcc and hcp stacking sequences, respectively, at different distances from the surface [29]. The agreement between the experimental data and the calculated density of states is remarkable. Even the relative intensity of the LDOS of fcc and hcp films in the calculations is conserved in the experimental results. The stacking sequence of Co films can be modified by choosing certain growth procedures such as the use of surfactants [34], pulsed laser deposition [35] or coevaporation.

References

[1] Prinz G A 1998 *Science* **282** 1660
[2] GMR
[3] Moodera J S, Kinder L R, Wong T M and Meservey R 1995 *Phys. Rev. Lett.* **74** 3273
[4] Monsma D J, Lodder J C, Popma Th J A and Dieny B 1995 *Phys. Rev. Lett.* **74** 5260
[5] Monsma D J, Vlutters R and Lodder J C 1998 *Science* **281** 407
[6] Rippard W H and Burhman R A 2000 *Phys. Rev. Lett.* **84** 971
[7] Chambliss D D, Wilson R J and Chiang S 1991 *Phys. Rev. Lett.* **66** 1721
    Stroscio J A *et al* 1992 *J. Vac. Sci. Technol.* A **10** 1981
    Voitgländer B, Meyer G and Amer N M 1991 *Phys. Rev.* B **44** 10 354
[8] Camarero J, Ferrón J, Cros V, Gómez L, Lázquez de Parga A L, Gallego J M, Prieto J E, de Miguel J J and
    Miranda R 1998 *Phys. Rev. Lett.* **82** 467
[9] See Besenbacher F, Pleth Nielsen L and Sprenger P T 1997 *The Chemical Physics of Solid Surfaces and
    Heterogeneous Catalysis* ed D A King ch 10
[10] Amar J G and Family F 1995 *Phys. Rev. Lett.* **74** 2066
[11] Hernán O S, Vázque de Parga A L, Gallego J M and Miranda R 1998 *Surf. Sci.* **415** 106
[12] Sánchez O, Gallego J M, Vázquez de Parga A L and Miranda R 1998 *Appl. Phys.* A **66** S1117
[13] Miranda R and Gallego J M 2001 *Phys. Rev.* B in press
[14] Fischer B *et al* 1997 *Surf. Sci.* **389** 366
[15] Hrbek J *et al* 1997 *Surf. Sci.* **389** L1002
[16] Miranda R 1993 *Phys. Scr.* T **49** 579
[17] de la Figuera J, Prieto J E, Ocal C and Miranda R 1993 *Phys. Rev.* B **47** 13 043
[18] de la Figuera J, Huerta-Garnica M A, Prieto J E, Ocal C and Miranda R 1995 *Appl. Phys. Lett.* **66** 1006
[19] de la Figuera J, Prieto J E, Ocal C and Miranda R 1994 *Surf. Sci.* **307–9** 538
[20] Gómez L and Diep T H 1995 *Phys. Rev. Lett.* **74** 1807
[21] Gómez L, Slutzky C, Ferrón J, de la Figuera J, Camarero J, Vázquez de Parga A L, de Miguel J J and Miranda R
    2000 *Phys. Rev. Lett.* **84** 4397
[22] Passeggi M C G Jr, Prieto J E, Miranda R and Gallego J M 2000 *Surf. Sci.* **462** 45
[23] Voitgländer B, Meyer G and Amer N M 1991 *Phys. Rev.* B **44** 10 354
[24] Sander D *et al* 1998 *Surf. Sci.* **402–4** 351
[25] Schmidt A K *et al* 1996 *Phys. Rev. Lett.* **77** 2977
[26] Ascolani H, Cerdá J R, de Andrés P L, de Miguel J J, Miranda R and Heinz K 1996 *Surf. Sci.* **345** 320
[27] Blum V *et al* 1999 *Phys. Rev.* B **59** 15966
[28] Vázquez de Parga A L, Vidal F J and Miranda R 2000 *Phys. Rev. Lett.* **85** 4365
[29] Stiles M D 1999 *J. Appl. Phys.* **79** 5805
[30] Müller S, Kostka G, Schäfer T, de la Figuera J, Prieto J E, Ocal C, Miranda R, Heinz K and Müller K 1996 *Surf.
    Sci.* **352–354** 46
[31] Camarero J *et al* 1999 *Appl. Phys.* A **69** 553
[32] Camarero J 1999 *PhD Thesis* UAM
[33] Math C, Braun J and Donath M 2001 *Surf. Sci.* **482–485** 556
[34] Camarero J, Spendeler L, Schmidt G, Heinz K, de Miguel J J and Miranda R 1994 *Phys. Rev. Lett.* **73** 2448
[35] Shen J *et al* 1998 *Phys. Rev. Lett.* **80** 1980